




Article

# The Adaptability of Cities to Climate Change: Evidence from Cities' Redesign towards Mitigating the UHI Effect

Georgia Spyrou <sup>1</sup>, Byron Ioannou <sup>1</sup> , Manolis Souliotis <sup>2</sup> , Andreas L. Savvides <sup>3</sup> and Paris A. Fokaides <sup>4,5,\*</sup> 

<sup>1</sup> Department of Architecture, Frederick University Cyprus, 7, Frederickou Str., Nicosia 1036, Cyprus

<sup>2</sup> Department of Chemical Engineering, University of Western Macedonia, Bakola & Sialvera, 50132 Kozani, Greece

<sup>3</sup> Department of Architecture, University of Cyprus, P.O. Box 20537, Nicosia 1678, Cyprus

<sup>4</sup> School of Engineering, Frederick University Cyprus, 7, Frederickou Str., Nicosia 1036, Cyprus

<sup>5</sup> Faculty of Civil Engineering and Architecture, Kaunas University of Technology, Studentų Str., 51367 Kaunas, Lithuania

\* Correspondence: eng.fp@frederick.ac.cy or paris.fokaides@ktu.lt

**Abstract:** The urban heat island effect can be studied through satellite imaging, field measurements, or analytical and numerical tools. However, the latter methods are considered more comprehensive due to the complexity of the built environment and the large quantity of data required for an adequate analysis. This study aims to investigate the extent to which specific urban bioclimatic design concepts and strategies affect the urban heat island intensity in Mediterranean semi-arid environmental conditions, classified as subtropical. The case study site chosen was Kaimakli, an urban district in Nicosia, Cyprus, known for high urban heat island intensities due to its location and rapid growth characterized by more impervious materials and less green vegetation. The analysis of the specific site considers parameters such as urban density, vegetation, soil sealing effect, building age and materials, land coverage ratio, and orientation. A design scenario consisting of three mitigation policies of different building types, heights, and vegetated types was developed and investigated. The study found that under semi-arid conditions, the use of extensive vegetation in an urban block of a 200 × 200 m<sup>2</sup> area and the reduction of the built area by about 10% resulted in an air temperature reduction of 1.5 °C during the summer solstice at 3:00 pm. These findings quantify the impact of specific urban heat island mitigation practices on decreasing the intensity of the effect under subtropical climatic conditions. This study provides valuable insights into the potential of specific urban bioclimatic design concepts and strategies to mitigate the urban heat island effect. The use of extensive vegetation and a reduction in the built area have been shown to be effective in reducing air temperatures, which can have significant implications for public health, energy consumption, and overall urban sustainability.

**Keywords:** urban heat island effect; urban planning; mitigation; microclimate model; computational analysis



**Citation:** Spyrou, G.; Ioannou, B.; Souliotis, M.; Savvides, A.L.; Fokaides, P.A. The Adaptability of Cities to Climate Change: Evidence from Cities' Redesign towards Mitigating the UHI Effect. *Sustainability* **2023**, *15*, 6133. <https://doi.org/10.3390/su15076133>

Academic Editor: Andrei P. Kirilenko

Received: 27 December 2022

Revised: 25 March 2023

Accepted: 28 March 2023

Published: 3 April 2023



**Copyright:** © 2023 by the authors. Licensee MDPI, Basel, Switzerland. This article is an open access article distributed under the terms and conditions of the Creative Commons Attribution (CC BY) license (<https://creativecommons.org/licenses/by/4.0/>).

## 1. Introduction

Urban heat islands occur when cities replace natural land cover with dense concentrations of pavement, buildings, and other surfaces that absorb and retain heat [1], resulting to an urban area that is significantly warmer than its surrounding rural areas [2]. This effect increases energy costs, air pollution levels, and heat-related illness and mortality [3]. In view of the continues efforts to mitigate the Urban Heat Island (UHI) Effect, numerous policies have been adopted in recent years which include financial incentives [4], remote working [5], and the reduction of the energy performance of buildings [6,7]. Extensive research in recent decades proved that urban climates and heat islands are diverse and related to various features; some of them are more local and others, universal. Bouvert et al. [8], Santamouris [9], and Li et al. [10] summarize the causes of UHI: less evapotranspiration

because of soil sealing; the reduced albedo of the surface results to solar energy absorption; for the same reason, as well as due to the high density of the buildings in urban blocks, the infrared radiative loss of the city during the night is also reduced; the reduced velocity of the air which is caused by the city surface terrain also leads to the reduction of convection; also, the human factor and the heat rejections from air-conditioning devices lead to a significant anthropogenic thermal load. It is obvious that these interactions are complex on their own. It is clear that the urban design demands and principles are affecting all of the above; urban development is, by definition, increasing soil sealing, albedo of the traditional building materials are low, densities are desirable and related to development feasibility, and constructions and buildings usually produce a rough urban surface [11]. Mitigation tools are usually trying to balance between the demand for less UHI but without compromising the functionality and the amenity of the build environment. Mitigation strategies are grouped in three sets of tools: urban morphology and geometry; soil sealing and green; and building and surface materials.

The first set of mitigation tools applies to the initial design principles or planning restrictions that produce the geometries of urban space. What is the climate performance of urban morphology in terms of coverage, building block volumes, and heights in relation to the open spaces, their orientation, and their insolation capacity [1,12]? Do urban canyons and layout settings facilitate cooling, especially at night [13]?

The second set has to do with soil sealing and the management of greening and trees. The benefits of trees and unsealed soil have been extensively investigated by many researchers for both their thermal and social aspects [9,14,15]. The process of evapotranspiration allows solar radiation to transform into latent heat, as a tree can withhold around 75% of the solar radiation that it receives. Greenery can also reduce longwave radiation between buildings [16,17]. Layout design decisions can increase unsealed soil and provide the minimum necessary hard surfaces for vehicle movement or other uses, maximizing natural soil surfaces.

The third but equally important set of mitigation strategies is related to the construction materials and mainly their external surfaces, as well as their heat capacity. Albedo is a surface indicator that shows what part of the energy from the sunlight reflects into the atmosphere. High albedo means high reflectivity, when it is combined with materials with low heat capacity, heat trapping from solar radiation is minimized [18,19]. However, in cases where the use of low thermal capacity materials is not desirable, there are strategies for smart heat storage; for example, humid soil or water (heat capacity =  $4.2\text{ J}/(\text{cm}^3 \cdot \text{K})$ ) could absorb heating and release it gradually through evaporation [9,20].

UHI may be investigated either by using images from satellites, by conducting measurements in the field, or with the development of models, analytical or numerical. On some occasions, qualitative practices are also employed to perform the analysis of the UHI effect. Before taking decisions on the mitigation practices of the phenomenon, a good practice is to perform the testing and validation of computational models which were especially developed for this purpose [21]. ENVI-met serves this specific purpose well—i.e., the pre-validation and the evaluation of proposed UHI mitigation strategies—by providing the ability to document and simulate the microclimate conditions in very high detail [22]. ENVI-met is a 3D microclimate simulation software used for a wide range of applications including urban planning, building design, and energy efficiency, considering multiple climate parameters. ENVI-met can simulate a variety of climate conditions, including day- and night-time temperatures, humidity, wind speed, and solar radiation in cities. It can also simulate the effects of different building materials, such as glass and stone, on the climate of the surrounding environments [23].

Empirical validation (in situ temperature observations) of the ENVI-met modelling results in the current situation can also be useful in cases where one or several of the examined development scenarios are physically constructed. In any case, ENVI-met enables the understanding of the contribution of different building elements and materials to this phenomenon

and, particularly, how they affect the urban microclimate. This application also enables the assessment of heat transfer between the indoor and the outdoor microclimate [24].

The local conditions in Cyprus have boosted UHI in recent decades. The semi-arid climate conditions, especially at the central plane where Nicosia, the capital of the island, is located, include heat waves, especially during the extended summer periods [25]. The plot-to-plot urban development patterns, the specifications regarding coverage, building volumes and heights, and the fragmentation of the open spaces have negatively influenced the issue. Water shortage, lifestyle choices, and inadequate planning have minimized the presence of private and public green spaces in the city [26,27]. The extensive asphalt road network, the predominance of concrete structures, and the use of materials of low albedo and high heat capacity have also increased UHI [28,29].

It is obvious that large-scale mitigation measures are hard to implement for the whole city of Nicosia and their results are applicable for the short-term. The extended urban sprawl and the large number of urban voids in every urban district [26] may provide the opportunity for the future diffusion of UHI-improved developments that would eventually reap benefits on a large scale in the long term. New building developments that adopt mitigation strategies and offer microenvironments with a better performance regarding UHI could be pilots for new urban design and building development approaches.

## 2. Materials and Methods

The purpose of this study is to investigate whether mitigation strategies at the micro scale of a private development complex could adequately affect the UHI effect. An area of 200 m × 200 m at the edge of the Kaimakli urban district [30] was strategically selected for a comparative UHI simulation. The selected area purposely includes both existing conventional plot-to-plot developments at its east site and an empty field/plot (temporarily given to agricultural use) of approximately 1.5 hectares to the west site. The existing building plot ratio at the area is 1.2, a fact that allows a gross density of around 100 residents per hectare, which allows for an urban design that meets major economic [31], social [32], and environmental [33] challenges [34]. The simulation follows two steps:

- Investigation of the current UHI performance of the existing fabric and the nearby empty field;
- Investigation of the same area, with a new development proposed at the empty field at the west. The new development maintains similar scale, building densities, and coverage as the surrounding fabric. Several mitigation strategies also apply which include the following:
  - i. Coverage management, building volumes, and heights in relation to the open spaces and their orientation designed to minimize solar heat trapping;
  - ii. A dry stream as an existing natural feature is preserved and turned into a water feature; soil sealing is minimized, while greenery and trees are maximized;
  - iii. High albedo and low heat capacity materials are strategically used for pavements and external surfaces.

The comparative case study approach can indicate to which extent new urban developments that apply mitigation strategies can improve the UHI effect in relation to the existing built environment.

It should be noted that Envi-met, as any other software tool, may perform uncertainties relevant to the microscale assurance of its grid independency; in situ temperature observations could mitigate this risk [26]. Unfortunately, the assessment of building and development scenarios does not allow these kinds of checks.

### 2.1. Investigated Site

The purpose of this study is the investigation of the Urban Heat Island (UHI) features and the evaluation of their magnitude in the context of an urban area in Kaimakli, Nicosia, with the use of the ENVI-met V5 software. The weather conditions of the analysis aimed to represent the conditions under a heat wave in Nicosia. In Nicosia, high UHI intensities

have been documented in the past due to the city's location as well as the fact that the city is constantly growing; the use of materials such as concrete and bricks help the UHI effect [27]. The simulated zone includes a combined built-up and vegetated area. Figure 1 presents an aerial view of the studied area.



**Figure 1.** Aerial view of the studied area.

The properties of the impervious materials and plants are provided in Table 1. Absorption concerns the fraction of shortwave radiation absorbed by the material; reflection refers to the fraction of shortwave radiation reflected by the material (Albedo); and emissivity concerns the longwave thermal radiation.

**Table 1.** Properties of impervious materials and plants.

| Parameter                     | Buildings | Asphalt | Soil | Pavements | Trees |
|-------------------------------|-----------|---------|------|-----------|-------|
| Absorption                    | 0.7       | 0.8     | 0.6  | 0.6       | 0.8   |
| Reflection                    | 0.3       | 0.2     | 0.4  | 0.4       | 0.2   |
| Transmittance                 | -         | -       | -    | -         | 0.3   |
| Emissivity                    | 0.9       | 0.9     | 0.9  | 0.9       | -     |
| Plant Height [m]              | -         | -       | -    | -         | 5     |
| Specific Heat [J/kg °C]       | 1100      | -       | -    | -         | -     |
| Thermal Conductivity [W/m °C] | 0.5       | -       | -    | -         | -     |
| Density [kg/m <sup>3</sup> ]  | 1500      | -       | -    | -         | -     |

The simulation was conducted for two different case studies:

- The baseline scenario presents the current status of the investigated area, with conventional construction and materials and more impervious surfaces with no vegetation or trees;
- The green scenario includes impervious surfaces and vegetation. In this advanced design scenario, more bioclimatic design elements, building types and heights, as well as vegetated types, pervious surfaces, and vegetation were included.



The analysis considered Kaimakli, a large northeastern suburb of Nicosia, with a population of 11,564 and an average elevation of 162m [30], near the old walled city of Nicosia. The climate of this suburb is similar to the city of Nicosia, which is subtropical semi-arid. The annual precipitation of Kaimakli is low. In the city, hot and dry summers, as well as cool-to-mild winters are observed. The rainfall mainly occurs in the winter. The average high temperature in summer is 37.2 °C and the low temperature is 22 °C. The average high temperature in winter is 22.2 °C and the low temperature is 5.7 °C. A synopsis of the climatic conditions at the Kaimakli area [35] is given in Figures 2 and 3, which show graphical representations of the extracted data from the PV GIS tool.

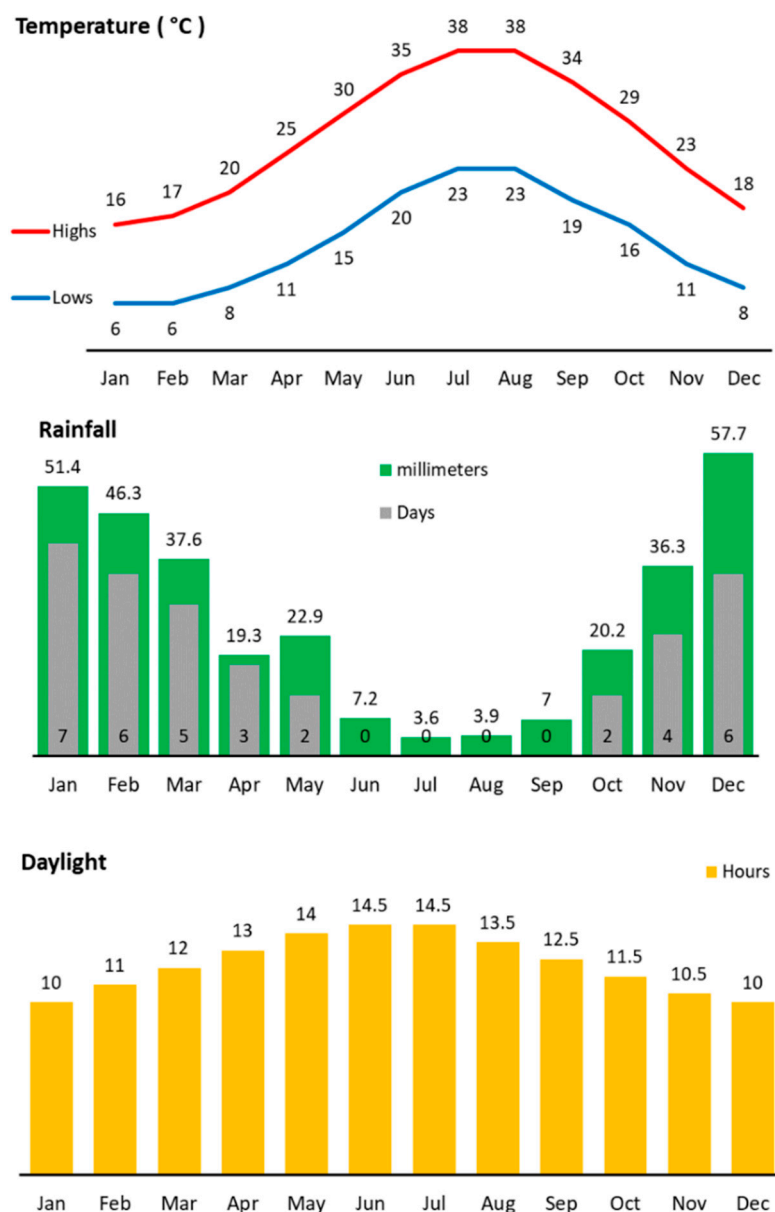
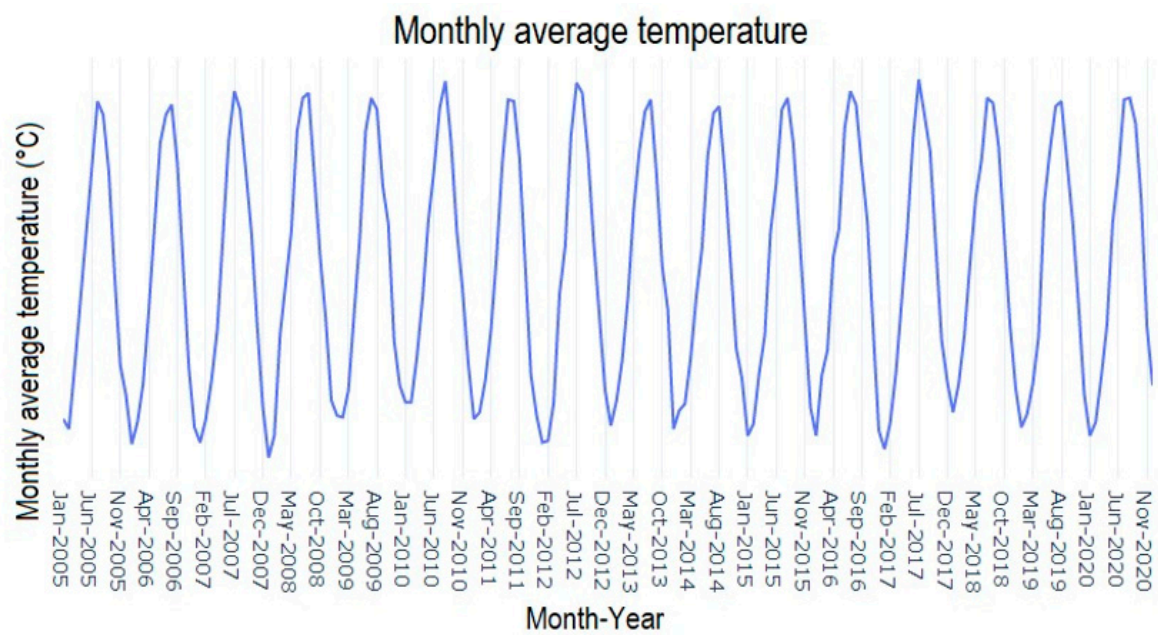


Figure 2. Climatic Conditions—Kaimakli Nicosia [35].

Table 2 and Figure 4 displays temperature measurements taken on a specific day during the simulation, as well as corresponding temperature data from the nearest weather station in Athalassa. Figure 5 illustrates the precise location of the weather station on a map.



**Figure 3.** Twenty-four-hour average temperature (°C).

**Table 2.** Simulated and Athalassa weather station temperatures for a specific day (°C).

| Date               | T, ENVI-met (°C) | T, Station (°C) | Deviation (%) |
|--------------------|------------------|-----------------|---------------|
| 23 June 2022 0:00  | 27.69            | 26.3            | 5%            |
| 23 June 2022 1:00  | 26.15            | 25.8            | 1%            |
| 23 June 2022 2:00  | 24.62            | 25.7            | 4%            |
| 23 June 2022 3:00  | 23.08            | 25.4            | 9%            |
| 23 June 2022 4:00  | 21.54            | 24.9            | 13%           |
| 23 June 2022 5:00  | 20               | 24.3            | 18%           |
| 23 June 2022 6:00  | 21.82            | 23.7            | 8%            |
| 23 June 2022 7:00  | 23.64            | 26.3            | 10%           |
| 23 June 2022 8:00  | 25.45            | 29.4            | 13%           |
| 23 June 2022 9:00  | 27.27            | 31.9            | 15%           |
| 23 June 2022 10:00 | 29.09            | 32.6            | 11%           |
| 23 June 2022 11:00 | 30.91            | 33.1            | 7%            |
| 23 June 2022 12:00 | 32.73            | 35.5            | 8%            |
| 23 June 2022 13:00 | 34.55            | 34.5            | 0%            |
| 23 June 2022 14:00 | 36.36            | 35              | 4%            |
| 23 June 2022 15:00 | 38.18            | 36.7            | 4%            |
| 23 June 2022 16:00 | 40               | 35.9            | 11%           |
| 23 June 2022 17:00 | 38.46            | 35.9            | 7%            |
| 23 June 2022 18:00 | 36.92            | 34.3            | 8%            |
| 23 June 2022 19:00 | 35.38            | 32.8            | 8%            |
| 23 June 2022 20:00 | 33.85            | 29.8            | 14%           |
| 23 June 2022 21:00 | 32.31            | 28.3            | 14%           |
| 23 June 2022 22:00 | 30.77            | 27.6            | 11%           |
| 23 June 2022 23:00 | 29.23            | 27              | 8%            |

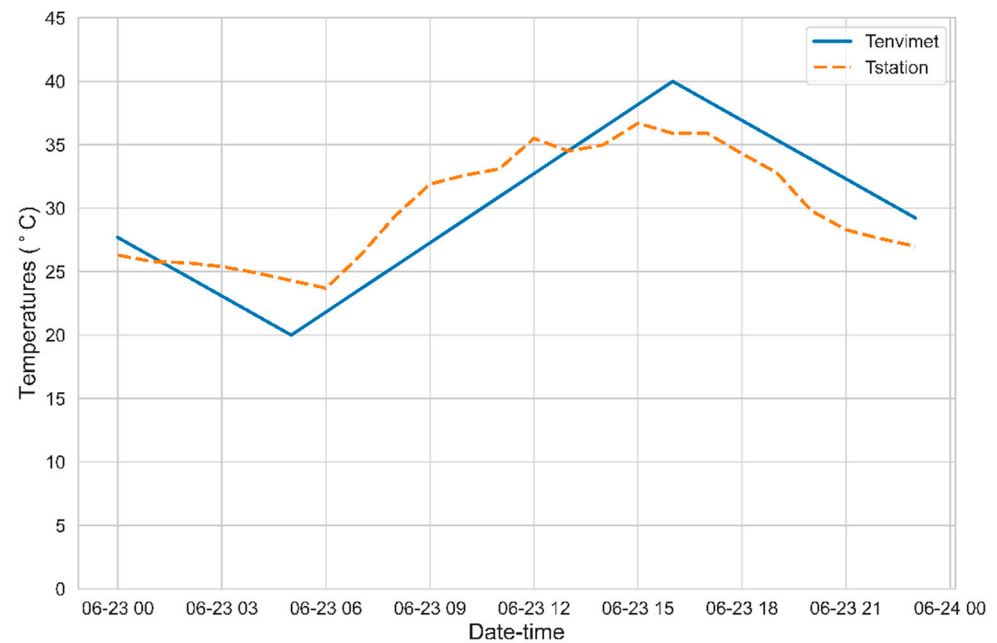


**Figure 4.** Simulated and Athalassa weather station temperatures for a specific day (°C).



**Figure 5.** Athalassa Radiosonde Station.

In the chosen area, a good presence of vegetation is shown around the house yard and trees along the street, while the area has a typical urban canyon layout: narrow streets and densely built structures.

Thirty-two buildings in total were considered in the model, ranging from 4 to 15 m height. Each of the two investigated cases had its own features, resulting mainly from the urban planning, the landscape, and the building materials. For the modelling of the vegetation, three different plant types were considered, namely, palm, olive, and citrus trees, which are considered as typical for the Mediterranean urban environment. Vegetation was observed mainly along the streets and in the house yards. The chosen plot area lies next to the buffer zone, in a densely built neighbourhood of Kaimakli, and combines both rural and urban features. The buildings in the considered plot are residential, both in apartment

blocks and detached single-family houses. An analysis of the built and the unbuilt spaces in the study area are presented in Figure 6, and Figure 7 provides an overview of the surface materials in the study area. In Figure 8, the panoramic view of the land use is given.

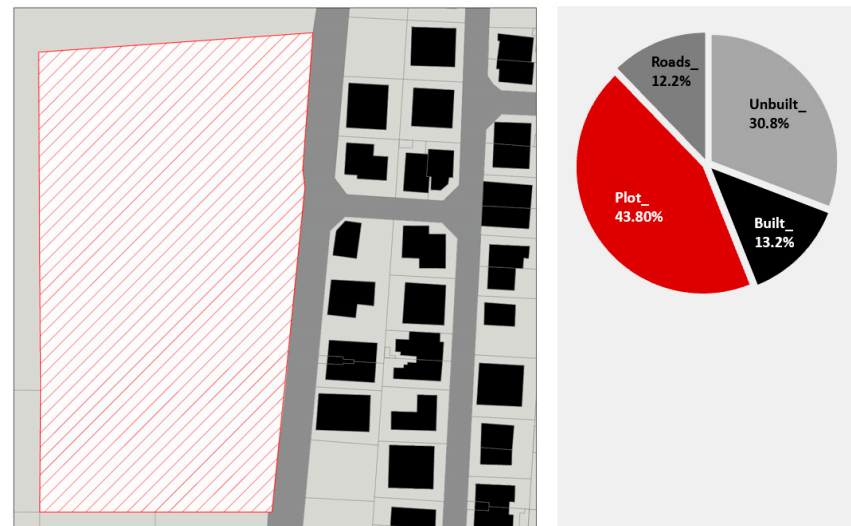


**Figure 6.** Built and un-built spaces analysis in the studied area.

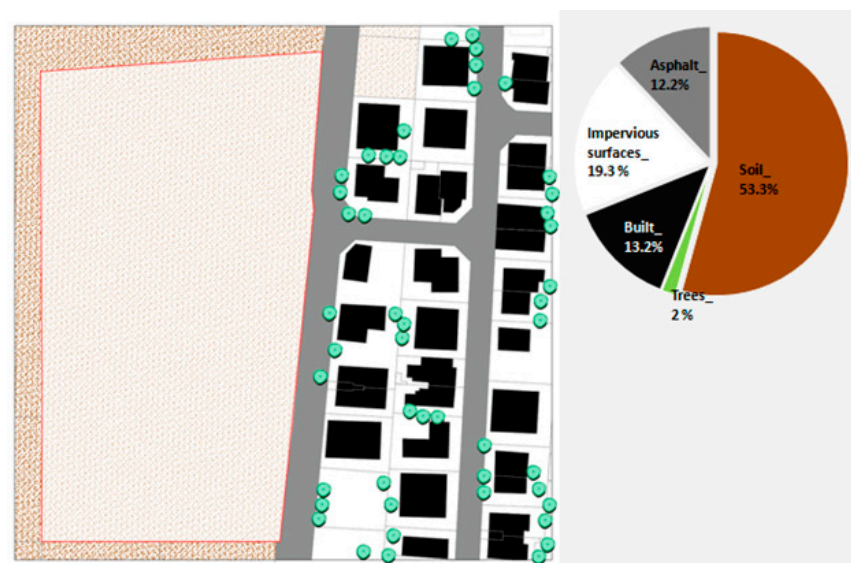


**Figure 7.** Surface materials analysis in studied area.

The proposed development concerns the design of 21 building blocks, with maximum heights of 15 m and minimum heights of 12 m. The plot was divided into three parts:

- Part A consisted of 10 building blocks, arranged in 'L' and 'U' shapes, open towards the south in order to allow maximum heat gain inside the buildings. The height of the buildings was 15 m. The land surface consisted of soil and paving materials, in order to identify differences between them. The trees faced west along the street. On the road between the buildings, two arrays of trees were placed at the southern and northern sides of the road, respectively. Under the specific case, the contribution of the trees to the mitigation of the high temperatures, caused by the impervious materials, was evaluated;
- Part B consisted of a green corridor, which included an array of trees, as well as a lake. The land surface consisted of soil, which was located in the middle of the plot, dividing the two types of buildings. This part was aimed at evaluating the impact of



- a green corridor on the plot and on the site area, and specifically at assessing whether using materials of high thermal mass helped to decrease the temperature;
- Part C consisted of 11 building blocks arranged around a square. The height of these buildings was assumed to be 12 m. The land surface consisted of soil and pavement materials, in order to identify the differences between them. The absence of trees was also taken into consideration. Based on this configuration, the interactions between the impervious and permeable soil surfaces were evaluated, as well as the temperature increase caused by the absence of trees.

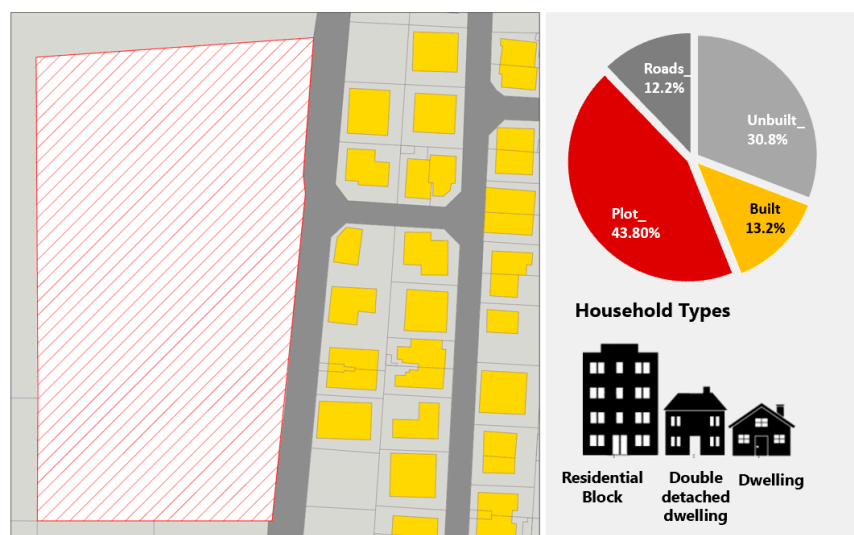


**Figure 8.** Land use analysis in studied area.

## 2.2. Computational Tool: ENVI-Met Model

ENVI-met is a three-dimensional microclimate modelling software designed to simulate the interactions between the built fabric surface, the natural landscape, and the atmosphere in urban environment [36]. ENVI-met simulates the evolution in time of selected thermodynamic parameters on a micro-scale, delivering multi-dimensional models of the interactions between the vegetation in urban areas and the atmosphere in the urban environment. The level of analysis of ENVI-met is the microclimate. The horizontal resolution of the analysis ranges between 0.5 m and 10m. Concerning the time step of analysis, this may vary from 1 to 5 s. The analysis is usually conducted between 24 and 48 h. ENVI-met is applying well established fundamentals of thermodynamics and fluid mechanics, with emphasis on the simulation of the interaction between the buildings and the environment, to deliver results which include the heat flow around and between buildings; the heat and humidity exchange at the soil level and between walls; thermohydrometric exchange in vegetation; and pollutant dispersion.

## 2.3. ENVI-Met Air Temperature Validation

The PVGIS system employs solar radiation data of a high quality derived from satellite imagery, alongside ambient temperature and wind speed data obtained from climate reanalysis models. The energy yield model undergoes validation based on measurements obtained from commercial modules tested at the European Solar Test Installation (ESTI), an ISO 17025-accredited photovoltaic calibration laboratory for all photovoltaic materials that operates under the Joint Research Centre (JRC). The PVGIS tool is utilized to extract monthly average historical data spanning.

The Athalassa Radiosonde Station is situated in a separate municipality; nonetheless, it represents the closest meteorological station available. Due to the lack of valid meteorological data at our site, the suggested validation process requires several months for

completion in order to ensure the eventual passage of appropriate dates. The dedicated section added provides, to an extent, a validation of the model.

Air temperatures that are significant for evaluating heat islands are those defined in the urban canopy. The urban canopy is defined as the area between the ground level and the dome of the buildings. They are most suitable for a study in which the goal is to moderate public health dangers, as they represent the most appropriate indicators of physical conditions essentially experienced by individuals. The height of the analysis was in accordance with the human level and the urban canopy level.

ENVI-met consists of the model groups below [37,38]:

- An atmospheric module, which computes air motion, 3-D turbulence, temperature, and relative humidity, taking into consideration obstacles (e.g., buildings, vegetation). The difference of radiation due to vegetation is also included in the analysis;
- A surface module, which analyses the emitted longwave and reflected shortwave radiation from diverse surfaces, taking into consideration the incident longwave and shortwave radiation. It reflects the albedo of the exteriors and shade as a function of the solar path and computes water vapor evaporation from the vegetation and transpiration from the soil, in view of the airflow-modifying effect of the vegetation. It is adapted to model flat surfaces;
- A vegetation module, which computes foliage temperature and the energy balance of the leaves, considering physiological and meteorological parameters;
- A soil module, which computes the thermo- and hydrodynamic processes that take place in the soil. This model considers the combination of the natural and artificial surfaces of the selected neighborhood, and it can also calculate heat exchange between a water body and its environment.

The area was rendered with a  $100 \times 100 \times 30$  (x-y-z) grid of 2 m each unit, with fixed spacing on the x- and y-axes, and a thicker grid near the ground, allowing a more accurate analysis of edge effects. The resolution was an average within the suggested values (for minimum 0.5 m to maximum 10 m). With the above constraints, a reasonable combination of accuracy and calculation time was achieved.

### 3. Results and Discussion

#### 3.1. Baseline Scenario

Figure 9 shows a map of the air temperatures at lower elevations (1.5 m from ground level) at 3 p.m. and 11 p.m. As expected, the road surfaces were the hottest zones, whereas the surroundings, which are less dense, experienced milder effects. The maximum temperature, from above the road surface, was 40 °C, while the minimum, recorded in densely vegetated areas, was 36.5 °C. Due to the northwesterly wind direction, the air temperature is relatively low. During the night, the air temperature decreases considerably compared to daytime temperatures. Due to the wind direction at night, air temperatures in a southeastern orientation were lower than in areas located in different orientations (lower than 30 °C, higher than 31 °C).

In Figure 10 the soil temperatures at 3:00 p.m. and 11:00 p.m. are depicted for the summer solstice. During the night, as expected, the soil temperature decreased considerably, compared to the day temperatures (maximum 33 °C, minimum 25 °C); however, the temperatures for the asphalt remained relatively high (above 31 °C). Indisputably, during the UHI effect, the temperature characteristics of dense street canyons are very distinct compared to those of rural or semi-urban areas. The narrower a street “canyon”, the less the potential insolation penetration to a street surface such as asphalt. On the other hand, in a less densely built fabric, the possibility of vegetation on larger areas of the ground surface increases. Hence, this affects both density and urban morphology. This observation is also due to the absorption and reflection of solar radiation in urban areas, the construction materials of high thermal mass, and also the emissivity (concrete, brick, asphalt, etc.). Therefore, from the simulation maps, it was concluded that in areas that impervious materials exist, such as soil, and in vegetated areas, the temperature is considerably lower

compared to areas represented by permeable surfaces. In addition, the orientation of buildings, trees, and other vegetation can contribute to the mitigation of UHIs. During the afternoon, at 1 p.m., the highest temperature was recorded for asphalt (above 55 °C), and the lowest temperatures were recorded around trees (below 30.5 °C). The existence of trees along the street decreased the temperature by 8 °C, as well as at the points where there were permeable surfaces, such as soil (14 °C lower than the asphalt surface). At the north orientations of buildings, the temperature was relatively low (30 °C) due to shade from the buildings and minimal solar radiation. For the buildings with a northern orientation, temperatures tend to be lower compared to the buildings oriented to the south; the same applies for the trees that face south. These results verify that both permeable surfaces and vegetation can reduce high urban temperatures and, consequently, the effects of heat islands.

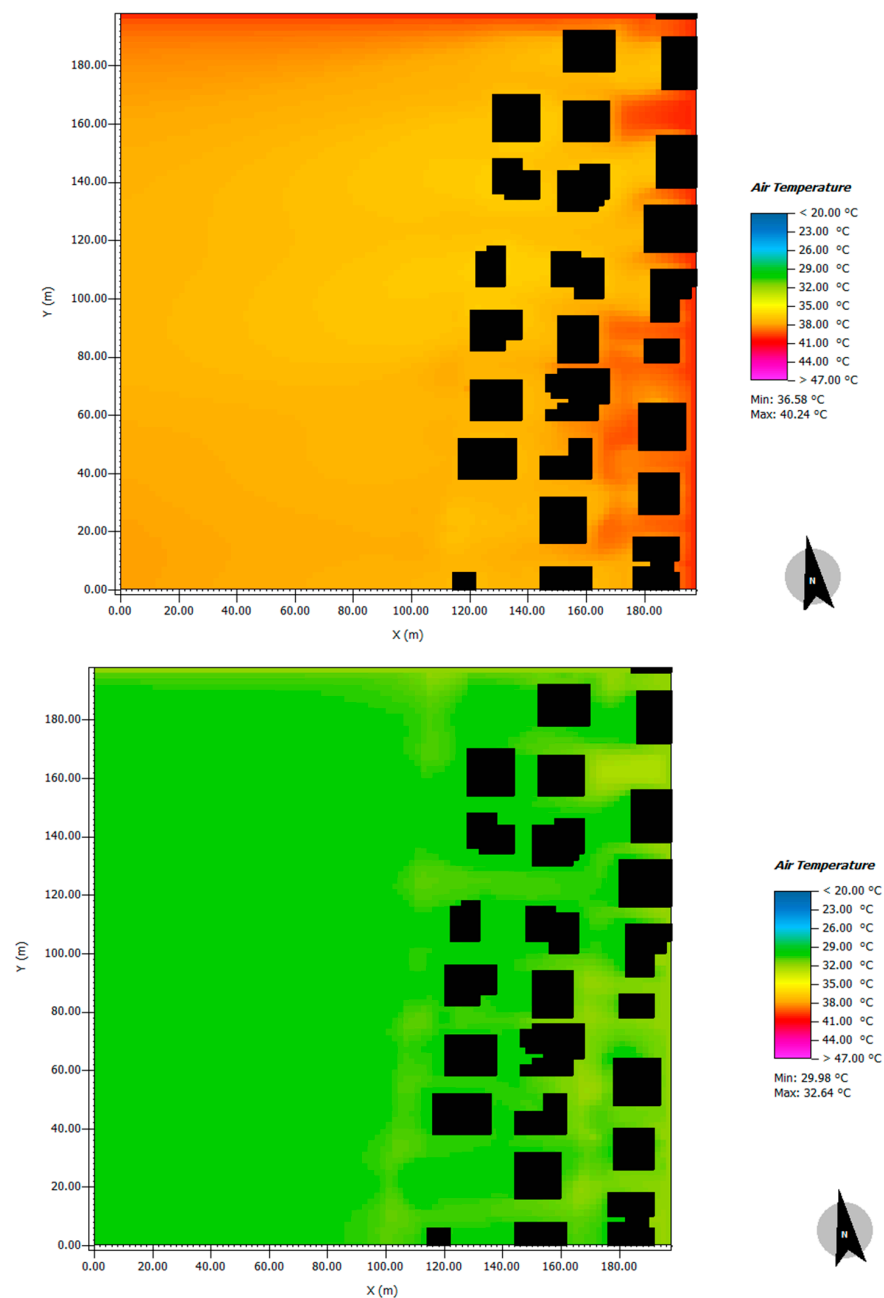


**Figure 9.** Baseline Scenario—air temperature at 1.5 m, 3:00 p.m. (above) and 11:00 p.m. (below), summer solstice; black shapes indicate buildings.

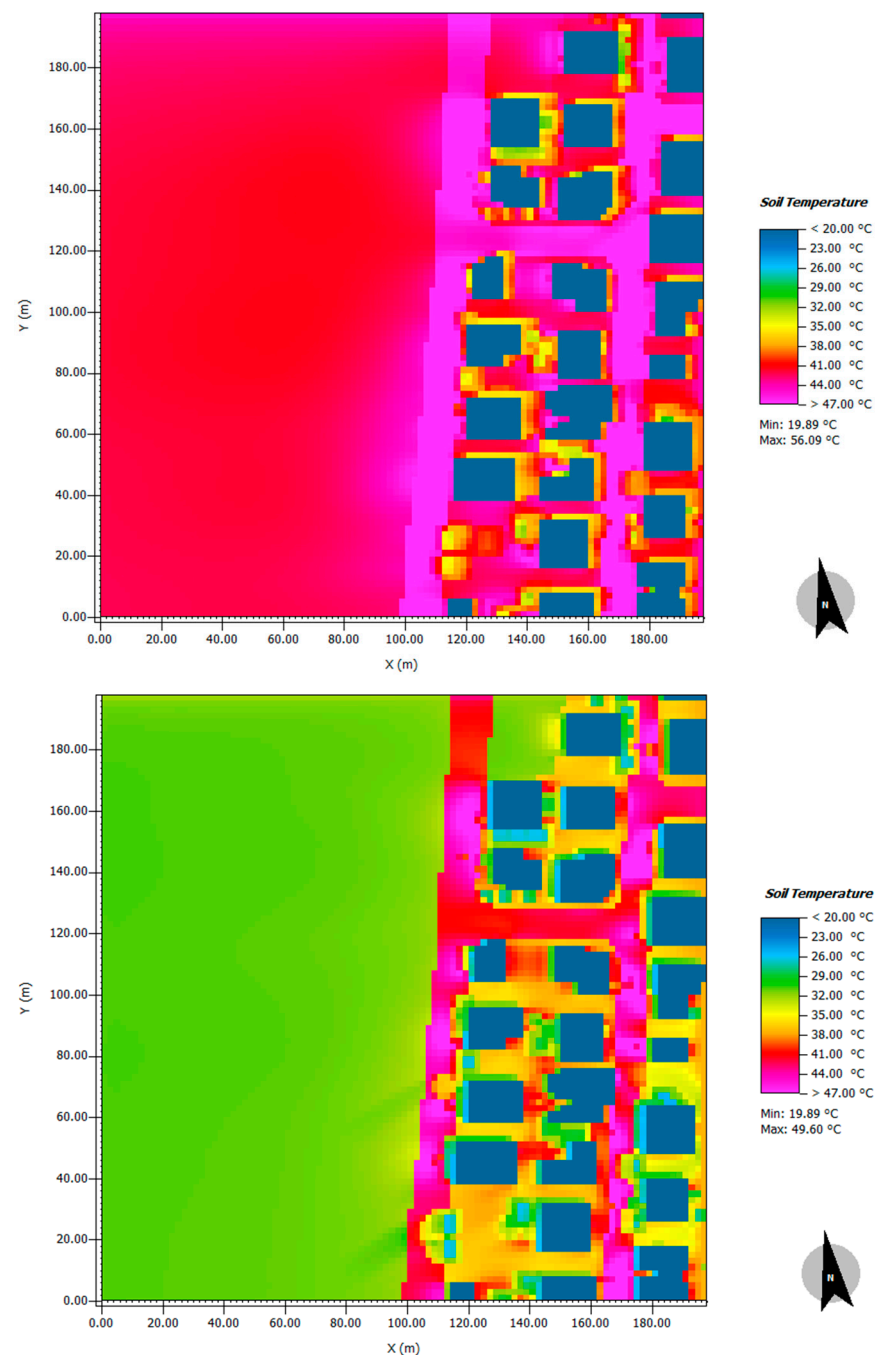


**Figure 10.** Baseline Scenario—soil temperature at 3:00 p.m. (above) and 11:00 p.m. (below), summer solstice.

### 3.2. Proposed Urban Development for the Unbuilt Area

A scenario was undertaken to assess and quantify the benefits that could result from the adoption of bioclimatic and sustainable design strategies for the investigated urban block. To evaluate the impact of the main requirements necessary to diminish urban microclimate effects, different vegetation strategies, building volumes and heights, soil sealing, and green spaces were considered for the same scenario.

Figure 11 illustrates the study area and the proposed development for the unbuilt area. In the proposed development, sustainable design strategies were pursued, such as a green corridor, trees along the street, green space, soil, and water surfaces. In addition, for certain points for the studied area, impervious surfaces without trees were proposed in order to evaluate the differences between impermeable and permeable materials.



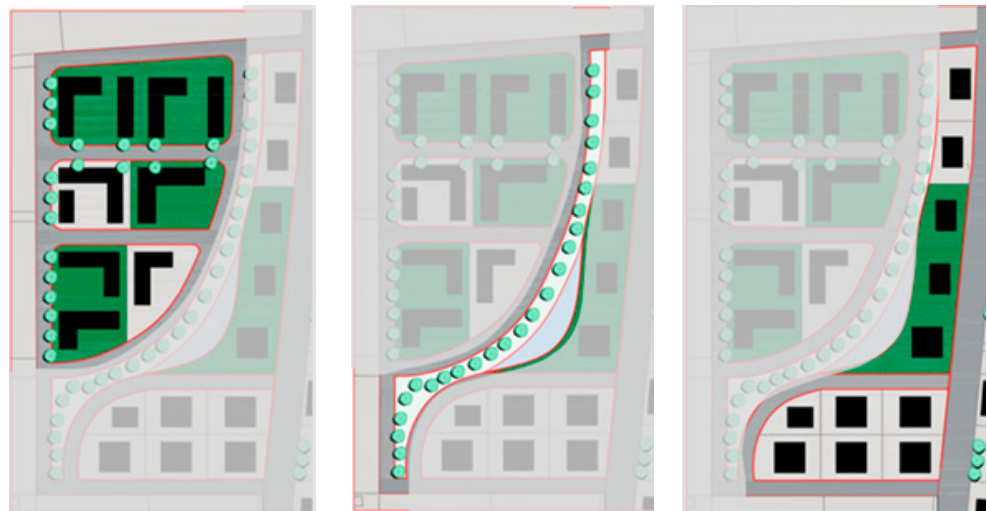


**Figure 11.** Proposed development for the unbuilt area: Part A (left), B (middle), and C (right).

The proposed development in the unbuilt area for Parts A, B, and C is presented in Figure 12 and presents the analysis of the percentage of buildings and surface material intended for the proposed development. The simulation was performed for 24 h during the summer and winter solstice. The analysis focused on the air temperature for land urban heat island, the canopy layer and soil temperature surface, the diffused solar radiation, and the albedo. Figure 13 presents the albedo for the proposed development around the unbuilt area. Albedo is the ratio of the amount of solar radiation reflected from a surface to the total amount reaching that surface. Albedo is measured on a scale of 0–1, with 0 being a surface of material that absorbs all the wavelengths of the solar radiation, and 1 meaning that a material reflects all the wavelengths of the solar radiation. According to Figure 13, the surface albedo of the asphalt is 0.15 to 0.2 and for the concrete is 0.4. Vegetated areas offer greater heat absorption, resulting in lower air temperatures. Conversely, asphalt and pavement absorb the solar radiation due to their low albedos, emitting it to the surroundings at night. This causes high values of air temperatures and UHI effect.

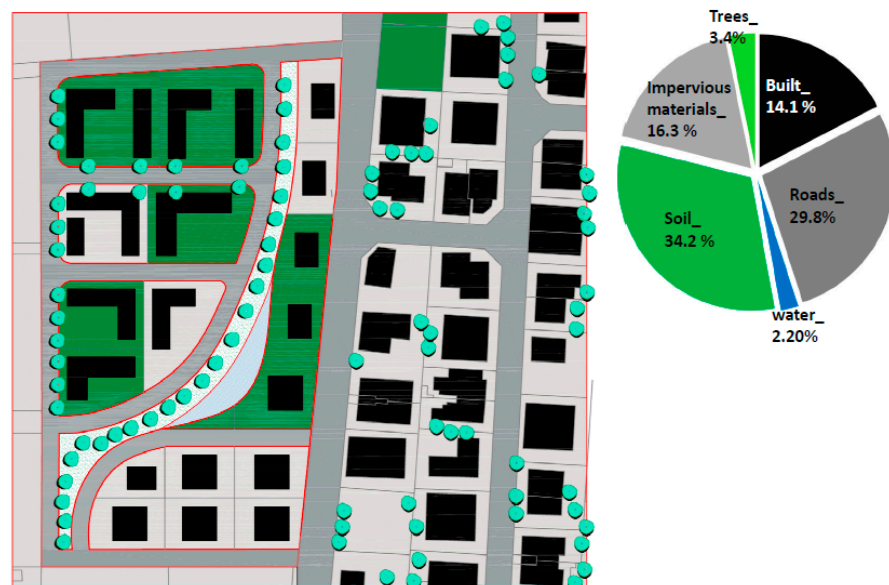


**Figure 12.** Percentage of buildings and surface materials analyzed for the proposed development.

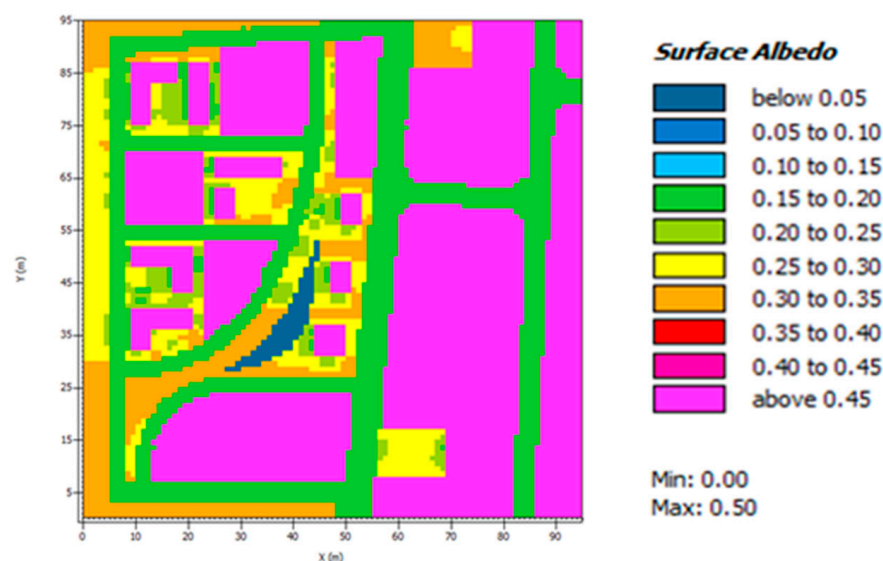
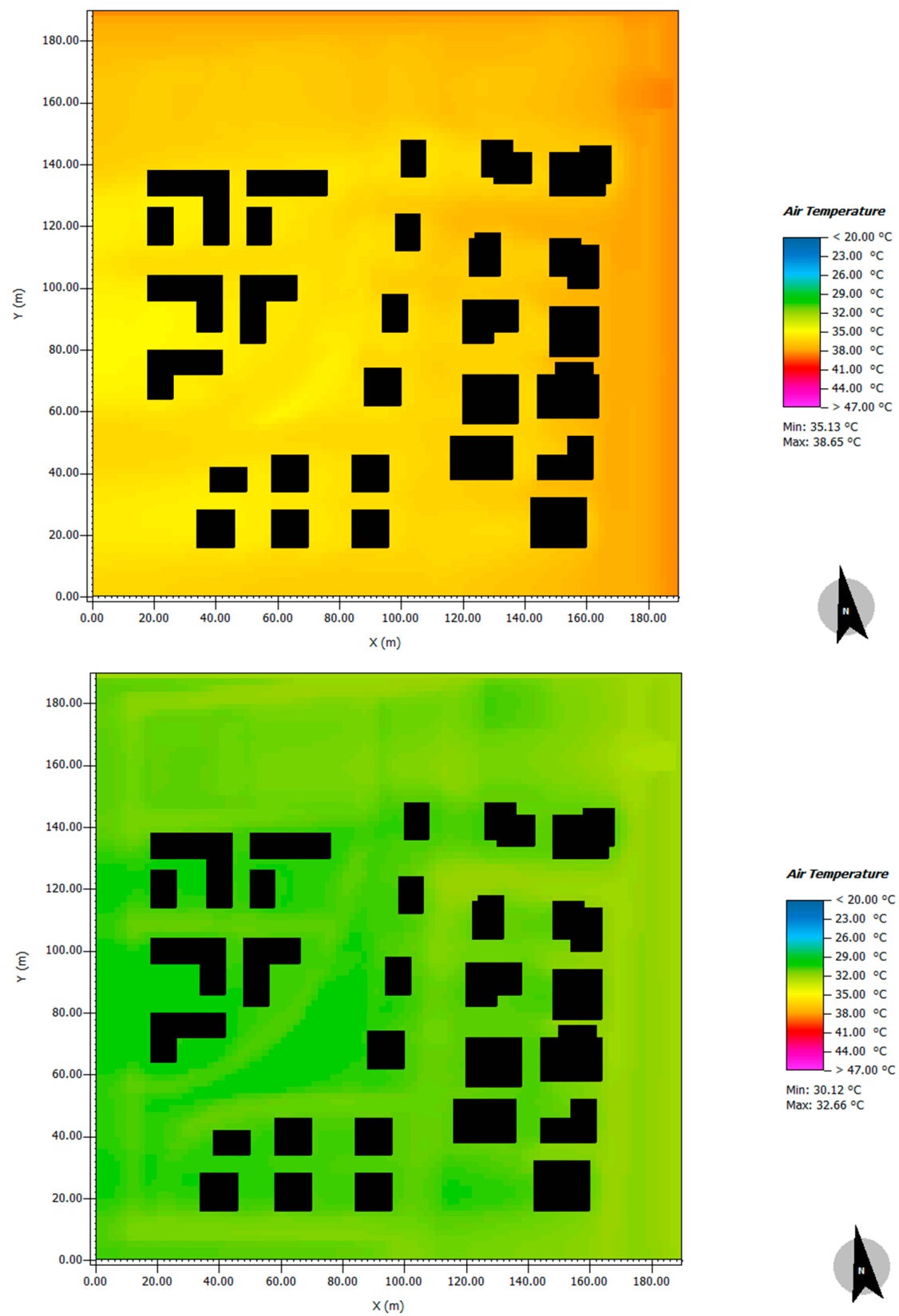


**Figure 13.** Albedo for the proposed development in the unbuilt area.

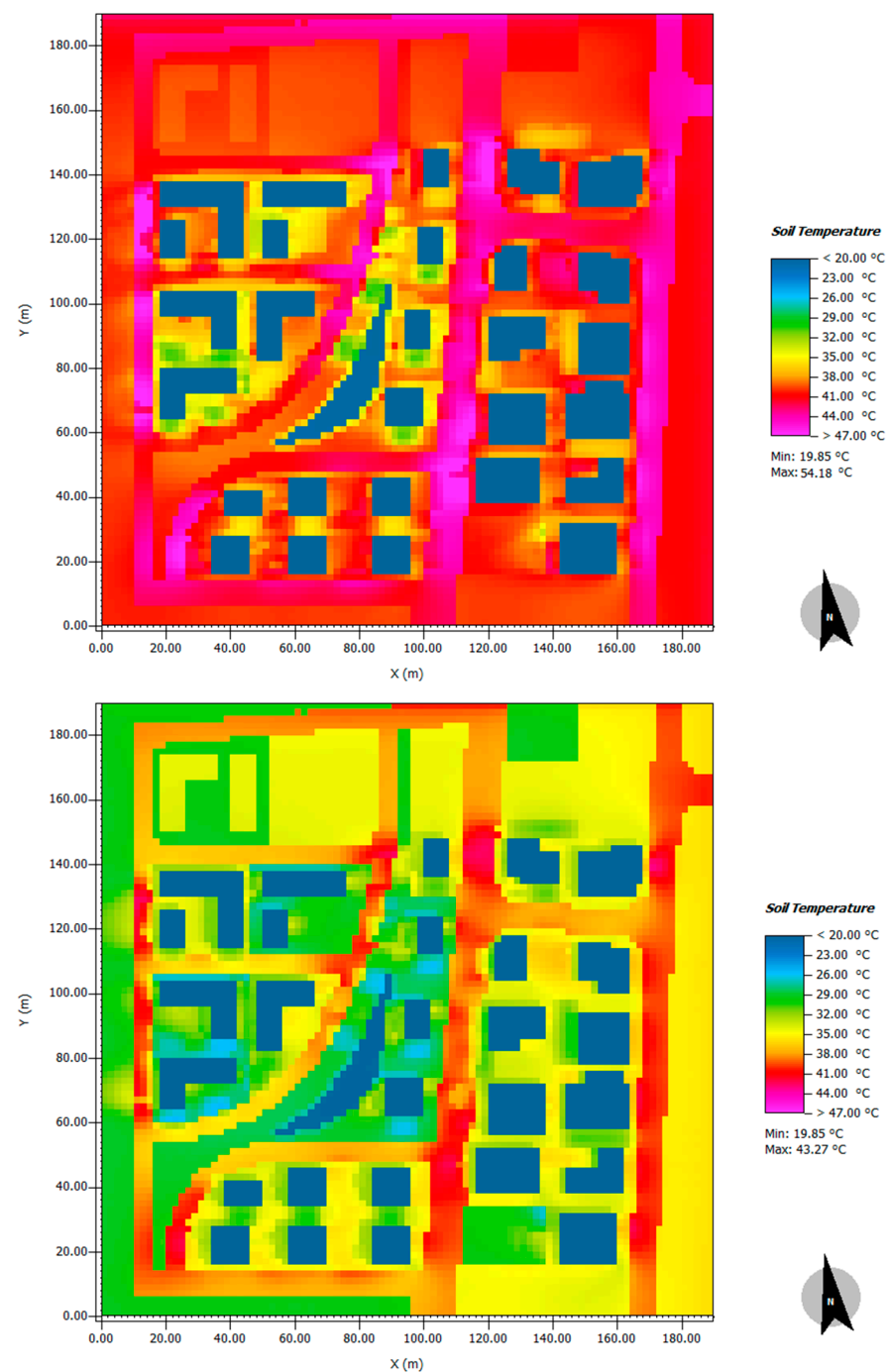
### 3.3. Urban Heat Island Effect for the Unbuilt Area for the Proposed Development

Figure 14 presents the air temperature for the proposed development in the unbuilt area at a level of 1.5 m height above land surface. During the day of Summer Solstice (21.06), the maximum temperature values were recorded from the road surfaces at 3 pm; as a result of the urban canyon layout. Areas that were less densely filled, with more vegetation and/or a water surface, experienced lower temperatures. The maximum temperature was 39.9 °C, while the minimum temperature, recorded from densely vegetated areas in the green corridor and at the water surface, was 35.6 °C. Thus, the maximum thermal gradient was 4 °C. For the agricultural land with exposed barren earth, the minimum temperature value was 36.6 °C and the maximum 38 °C. Compared to the current urban setup, the proposed development, with the green corridor and water, reported temperatures 1 °C lower over the newly developed area. Note that both setups serve the same density (approx. plot ratio 1:0). According to this value, it is confirmed that sustainable design strategies, as well as bioclimatic strategies, such as the green corridor and a water surface, can mitigate higher temperatures and also the UHI.

Figure 15 presents the temperature of the surface at the land level for the proposed development for the unbuilt area during the summer solstice. Surface temperatures are caused mainly by the emitted thermal energy of the land and the buildings. The soil temperatures were calculated at 3 pm. During the daytime, at the summer solstice, the maximum land temperature recorded for the streets and pavement surfaces was 54.1 °C, while the minimum temperatures for the soil surfaces, green spaces, and water was 30.1 °C. The temperature difference between the permeable and impermeable surfaces was about 24 °C. During the night, the temperature tended to be above 31.5 °C. For the green space and water, the minimum temperature recorded was 22.4 °C. The temperature difference between the high and low temperatures was 9.1 °C. Thus, it can be concluded that a high proportion of impervious surface, with differing radiative, thermal, and moisture properties, results in high temperatures. The temperature differences between the day and night were 24 °C and 9 °C, respectively. As a result, it can be verified that the use of permeable surfaces and vegetated areas can mitigate the high temperatures and also the UHI effect.



**Figure 14.** Air temperature for the proposed development in the unbuilt area, x–y view at  $z = 1.5$  m at 3:00 p.m., summer solstice (**above**); and 11:00 p.m., summer solstice (**below**); black shapes indicate buildings.



**Figure 15.** Soil surface temperature for the proposed development in the unbuilt area for summer solstice for 3 p.m. (above) and 11 p.m. (below).

#### 4. Conclusions

This study identifies several significant factors that contribute to the intensity of the urban heat island (UHI) effect. The increased urbanization, building density, geometry, and use of construction materials such as concrete and asphalt result in urban environmental degradation, particularly in the summer when high temperatures are prevalent. Moreover, the location and orientation of buildings also play a crucial role in determining air temperature. The study finds that the location of buildings and the creation of west-shadowed open spaces provide a milder air temperature for the most vibrant areas. The study area's results indicate that even in an average built-up area, an UHI effect can occur with high



temperature differences between built-up areas, open green spaces, and water surfaces. Consequently, the urban microclimate of the Kaimakli region has been significantly altered, and a fully developed UHI is possible. In conclusion, this study highlights the need to adopt sustainable and bioclimatic design strategies to mitigate the adverse impacts of urbanization on microclimates, soil processes, and human health.

Athalassa Radiosonde Station is situated in an undeveloped region; thus, adjustments were made to the data based on the findings of this study. These modifications serve to enhance the overall accuracy of the measurements [26]. One of the advantages of the followed methodology is that the case-study area combined two types of urban structures—the conventional development, which physically exists on site, and the future development scenario in which mitigation strategies were applied and will expand on an existing rural area. As concluded from this study, Figure 16 shows the air temperature in the urban area ranged at high levels during the hotter hours (above 40 °C); compared to the existing rural landscape in which the temperature varied at lower levels (36.5 °C), the temperature difference was almost 4 °C (Table 3). Of course, the downside of the current methodology is that the larger image at a city scale is missing, especially knowing that this area lies at the edge of the city and not in the center of a continuous built area. This shortcoming is mitigated by taken into consideration the conclusions of previous large-scale studies referring to the same area [22,39].

**Table 3.** Air temperature difference between baseline scenario and proposed development.

| Scenario  | Minimum Temperature (°C) | Maximum Temperature (°C) | Median Temperature (°C) |
|---|--------------------------|--------------------------|-------------------------|
| Baseline Scenario                                 | 36.58                    | 40.24                    | 37.64                   |
| Proposed urban development<br>in the unbuild area | 35.13                    | 38.65                    | 36.63                   |
| Air temperature difference                        | 1.45                     | 1.59                     | 1.01                    |

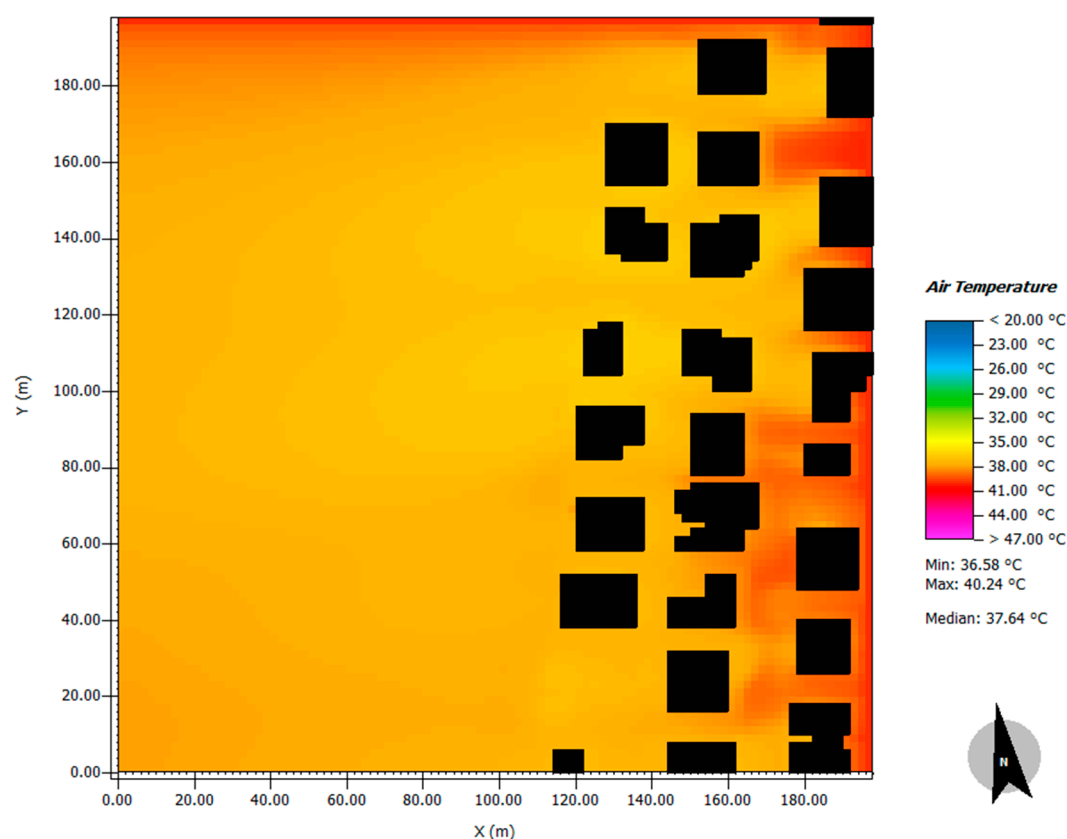


**Figure 16.** Cont.

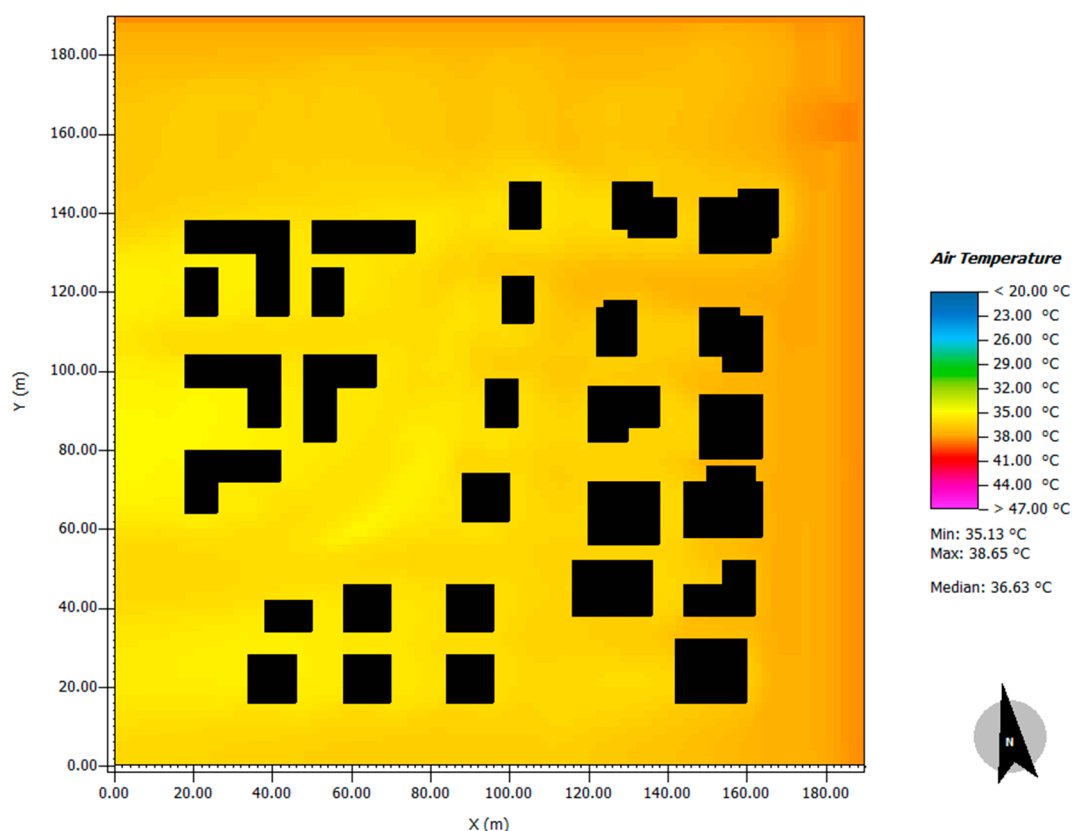


**Figure 16.** Air temperature difference between Baseline Scenario at 1.5 m, 3:00 p.m. (**above**); and for the proposed development in the unbuilt area at 3:00 p.m. (**below**), summer solstice; black shapes indicate buildings.

Indisputably, urban design and soil sealing are parameters that can either aggravate or mitigate the UHI phenomenon, observed in dense urban environments around the world. The soil surface during the day, recorded from impermeable surfaces such as asphalt and pavement, was above 55 °C, while in the permeable materials, such as soil, a lower temperature was recorded at 38.7 °C.

According to the analysis of the proposed development, there were differences of up to 9 °C from the early hours to night time during the summer solstice. The maximum air temperature was above 39 °C, while the maximum air temperature during the night was above 30 °C. The high proportion of impervious surface, with differing radiative properties, resulted in high air temperatures, compared to the surrounding rural landscape, which is typical of the UHI effect. At the canopy level, the air temperatures during the day and night during the summer and winter solstices varied near the same values for all areas, while the temperature differences were negligible (0.2 to 0.3 °C). The air temperature remained high during the day and night, at 35 °C and 30 °C, respectively. From these values, it can be concluded that increased impermeable surfaces, as well as the absence of open green spaces, can cause high values of elevated temperatures during all seasons.

Urban green spaces can mitigate the effects of UHIs by changing the surface energy balance of the system. Evapotranspiration from urban green spaces can cool leaf surfaces and air temperatures, as the energy from solar radiation can be stored as latent, rather than sensible heat. Vegetation cover and green roofs affect soil surface temperature; specifically, soils beneath trees and shrubs have lower summer temperatures than soils with impermeable surfaces. In Part A of the proposed development, the trees were placed in western orientations along the street. At a specific point on the road between the buildings, an array of trees was placed on the southern and northern sides of the road. For the summer solstice day, at points with existing trees, the elevated surface temperature of the

asphalt road could be decreased by about 7 °C (from 54.18 °C to 47.32 °C). This verifies the important contribution made by trees in the mitigation of high temperatures. Comparing temperatures between the green corridor and individual trees, it can be concluded that, in places where there are organized urban green spaces, temperatures tend to be lower. In Part B of the proposed development—the green scenario with a green corridor and an array of trees and soil and water surfaces—the temperature recorded was lower than that of the impermeable surfaces. The soil temperature difference between the vegetated area, water, and pavement surfaces during summer solstice was above 24 °C (54.18 °C to 30.17 °C), while during the daytime at the winter solstice, the difference was above 13 °C (25.7 °C to 39.4 °C). Another important parameter used to mitigate elevated temperatures is the shade from buildings and single trees. For these, the minimum temperature was below 30.4 °C at the summer solstice and below 23 °C for the winter solstice.

The absence of vegetated areas and increased impervious surfaces, such as asphalt and pavement, are the main factors that contribute to high air temperatures and urban heat island (UHI) effects. However, the proper landscaping of green spaces, building orientation, and sustainable and bioclimatic design strategies, including the use of permeable materials, soil, and vegetation, can help mitigate the UHI effect in urban areas. This study demonstrates that implementing bioclimatic design strategies can reduce the adverse impacts of urbanization on microclimates, soil processes, and human health. The findings highlight the importance of incorporating sustainable design practices in urban planning and development to mitigate the effects of urban heat islands and promote overall urban sustainability.

**Author Contributions:** Conceptualization, G.S. and B.I.; methodology, G.S. and B.I.; validation, M.S. and P.A.F.; formal analysis, M.S. and A.L.S.; investigation, G.S. and B.I.; resources, G.S. and A.L.S.; data curation A.L.S. and P.A.F.; writing—original draft preparation, G.S. and B.I.; writing—review and editing, M.S., A.L.S. and P.A.F.; visualization, G.S. and M.S.; supervision, P.A.F.; project administration, G.S. All authors have read and agreed to the published version of the manuscript.

**Funding:** This research received no external funding.

**Institutional Review Board Statement:** The study did not require ethical approval.

**Informed Consent Statement:** Not applicable.

**Data Availability Statement:** Not applicable.

**Conflicts of Interest:** The authors declare no conflict of interest.

## References

1. Santamouris, M.; Ding, L.; Osmond, P. Urban heat island mitigation. In *Decarbonising the Built Environment: Charting the Transition*; Springer: Berlin/Heidelberg, Germany, 2019; pp. 337–355.
2. Yang, J.; Santamouris, M. Urban Heat Island and Mitigation Technologies in Asian and Australian Cities—Impact and Mitigation. *Urban Sci.* **2018**, *2*, 74. [\[CrossRef\]](#)
3. Founda, D.; Santamouris, M. Synergies between Urban Heat Island and Heat Waves in Athens (Greece), during an extremely hot summer (2012). *Sci. Rep.* **2017**, *7*, 10973. [\[CrossRef\]](#) [\[PubMed\]](#)
4. Panteli, C.; Klumbyte, E.; Apanavičienė, R.; Fokaides, P.A. An overview of the existing schemes and research trends in financing the energy upgrade of buildings in Europe. *J. Sustain. Archit. Civ. Eng.* **2020**, *27*, 53–62. [\[CrossRef\]](#)
5. Kylili, A.; Afxentiou, N.; Georgiou, L.; Panteli, C.; Morsink-Georgalli, P.Z.; Panayidou, A.; Fokaides, P.A. The role of Remote Working in smart cities: Lessons learnt from COVID-19 pandemic. *Energy Sources Part A Recovery Util. Environ. Eff.* **2020**, 1–16. [\[CrossRef\]](#)
6. Fokaides, P.A.; Christoforou, E.A.; Kalogirou, S.A. Legislation driven scenarios based on recent construction advancements towards the achievement of nearly zero energy dwellings in the southern European country of Cyprus. *Energy* **2014**, *66*, 588–597. [\[CrossRef\]](#)
7. Fantozzi, F.; Gargari, C.; Rovai, M.; Salvadori, G. Energy Upgrading of Residential Building Stock: Use of Life Cycle Cost Analysis to Assess Interventions on Social Housing in Italy. *Sustainability* **2019**, *11*, 1452. [\[CrossRef\]](#)
8. Bouyer, J.; Musy, M.; Huang, Y.; Athamena, K. Urban Heat Island Effect by Urban Design: Forms and Materials. In *Cities and Climate Change: Responding to an Urgent*; AgendaHoornweg, D., Freire, M., Lee, M., Bhada-Tata, P., Yuen, B., Eds.; The Worldbank: Washington, DC, USA, 2012; Volume 2, pp. 164–181.

9. Santamouris, M. Urban Warming and Mitigation: Actual status, impacts and challenges. In *Urban Climate Mitigation Techniques*; Santamouris, M., Kolokotsa, D., Eds.; Earthscan: London, UK, 2016; pp. 1–26.
10. Li, X.; Zhou, Y.; Yu, S.; Jia, G.; Li, H.; Li, W. Urban heat island impacts on building energy consumption: A review of approaches and findings. *Energy* **2019**, *174*, 407–419. [\[CrossRef\]](#)
11. Moon, S.-Y.; Kim, J.; Chong, W.K.O.; Ariaratnam, S.T. Urban Green Space Layouts and Urban Heat Island: Case Study on Apartment Complexes in South Korea. *J. Urban Plan. Dev.* **2018**, *144*, 04018004. [\[CrossRef\]](#)
12. Zhou, Y.; Zhuang, Z.; Yang, F.; Yu, Y.; Xie, X. Urban morphology on heat island and building energy consumption. *Procedia Eng.* **2017**, *205*, 2401–2406. [\[CrossRef\]](#)
13. Sobstý, J.; Thorsten, E.; Abdolhosseini, M.; Ulm, F.-J.; Pellenq, R. Role of City Texture in Urban Heat Islands at Nighttime. *Phys. Rev. Lett.* **2018**, *120*, 108701. [\[CrossRef\]](#)
14. Gatto, E.; Buccolieri, R.; Aarrevaara, E.; Ippolito, F.; Emmanuel, R.; Perronace, L.; Santiago, J.L. Impact of Urban Vegetation on Outdoor Thermal Comfort: Comparison between a Mediterranean City (Lecce, Italy) and a Northern European City (Lahti, Finland). *Forests* **2020**, *11*, 228. [\[CrossRef\]](#)
15. Emmanuel, R.; Loconsole, A. Green infrastructure as an adaptation approach to tackling urban overheating in the Glasgow Clyde Valley Region, UK. *Landsc. Urban Plan.* **2015**, *138*, 71–86. [\[CrossRef\]](#)
16. Kohler, M.; Tannier, C.; Blond, N.; Aguejda, R.; Clappier, A. Impacts of several urban-sprawl countermeasures on building (space heating) energy demands and urban heat island intensities. A case study. *Urban Clim.* **2017**, *19*, 92–121. [\[CrossRef\]](#)
17. Roman, K.K.; O'Brien, T.; Alvey, J.; Woo, O. Simulating the effects of cool roof and PCM (phase change materials) based roof to mitigate UHI (urban heat island) in prominent US cities. *Energy* **2016**, *96*, 103–117. [\[CrossRef\]](#)
18. Hirano, Y.; Fujita, T. Evaluation of the impact of the urban heat island on residential and commercial energy consumption in Tokyo. *Energy* **2012**, *37*, 371–383. [\[CrossRef\]](#)
19. Morakinyo, T.E.; Balogun, A.A.; Adegun, O.B. Comparing the effect of trees on thermal conditions of two typical urban buildings. *Urban Clim.* **2013**, *3*, 76–93. [\[CrossRef\]](#)
20. Gemechu, F. Review of urban surface parameterizations for numerical climate models. *Urban Clim.* **2018**, *24*, 830–851.
21. Ramakrishnan, L.; Aghamohammadi, N.; Fong, C.S.; Ghaffarianhoseini, A.; Wong, L.P.; Noor, R.; Hanif, N.R.; Aziz, W.N.A.W.A.; Sulaiman, N.M.; Hassan, N. A qualitative exploration on the awareness and knowledge of stakeholders towards Urban Heat Island phenomenon in Greater Kuala Lumpur: Critical insights for urban policy implications. *Habitat Int.* **2019**, *86*, 28–37. [\[CrossRef\]](#)
22. Crank, P.J.; Sailor, D.J.; Ban-Weiss, G.; Taleghani, M. Evaluating the ENVI-met microscale model for suitability in analysis of targeted urban heat mitigation strategies. *Urban Clim.* **2018**, *26*, 188–197. [\[CrossRef\]](#)
23. ENVI-met. Calculate the Microclimate of a City Down to the Square Metre. 2023. Available online: <https://www.envi-met.com/> (accessed on 5 February 2023).
24. Salata, F.; Golasi, I.; de Lieto Vollaro, A.; de Lieto Vollaro, R. How high albedo and traditional buildings' materials and vegetation affect the quality of urban microclimate. A case study. *Energy Build.* **2015**, *99*, 32–49. [\[CrossRef\]](#)
25. Theophilou, M.; Serghides, D. Estimating the characteristics of the Urban Heat Island Effect in Nicosia, Cyprus, using multiyear urban and rural climatic data and analysis. *Energy Build.* **2015**, *108*, 137–144. [\[CrossRef\]](#)
26. Hadjimitsis, D.; Retalis, A.; Michaelides, S.; Tymvios, F.; Paronis, D.; Themistocleous, K.; Agapiou, A. *Satellite and Ground Measurements for Studying the Urban Heat Island Effect in Cyprus*, In *Remote Sensing of Environment: Integrated Approaches*; Hadjimitsis, D., Ed.; Intechopen: London, UK, 2013; pp. 1–24. [\[CrossRef\]](#)
27. Fokaides, P.A.; Kyli, A.; Nicolaou, L.; Ioannou, B. The effect of soil sealing on the urban heat island phenomenon. *Indoor Built Environ.* **2016**, *25*, 1136–1147. [\[CrossRef\]](#)
28. Cui, Y.; Yan, D.; Hong, T.; Ma, J. Temporal and spatial characteristics of the urban heat island in Beijing and the impact on building design and energy performance. *Energy* **2017**, *130*, 286–297. [\[CrossRef\]](#)
29. Guo, X.; Hendel, M. Urban water networks as an alternative source for district heating and emergency heat-wave cooling. *Energy* **2018**, *145*, 79–87. [\[CrossRef\]](#)
30. Kaimakli—Wikipedia Article. Available online: <https://en.wikipedia.org/wiki/Kaimakli> (accessed on 14 July 2018).
31. Miner, M.J.; Taylor, R.A.; Jones, C.; Phelan, P.E. Efficiency, economics, and the urban heat island. *Environment and Urbanization*. **2017**, *29*, 183–194. [\[CrossRef\]](#)
32. Mirzaei, P.A. Recent challenges in modeling of urban heat island. *Sustain. Cities Soc.* **2015**, *19*, 200–206. [\[CrossRef\]](#)
33. Halder, B.; Bandyopadhyay, J.; Banik, P. Monitoring the effect of urban development on urban heat island based on remote sensing and geo-spatial approach in Kolkata and adjacent areas, India. *Sustain. Cities Soc.* **2021**, *74*, 103186. [\[CrossRef\]](#)
34. Li, S.Y.; Han, J.Y. The impact of shadow covering on the rooftop solar photovoltaic system for evaluating self-sufficiency rate in the concept of nearly zero energy building. *Sustain. Cities Soc.* **2022**, *80*, 103821. [\[CrossRef\]](#)
35. National Oceanic and Atmospheric Association. Available online: <http://www.noaa.gov/climate-data-and-reports> (accessed on 14 July 2018).
36. EnviMET: Decoding Urban Nature. Available online: <https://www.envi-met.com/> (accessed on 14 July 2018).
37. Grifoni, R.C.; Sargolini, M.; D'Onofrio, R. *Quality of Life in Urban Landscapes*; Springer: Berlin/Heidelberg, Germany, 2018.



38. Szecs, Á. Wind comfort in a public urban space-case study within Dublin Docklands. *Front. Archit. Res.* **2013**, *2*, 50–66. [[CrossRef](#)]
39. Morini, E.; Touchaei, A.G.; Rossi, F.; Cotana, F.; Akbari, H. Evaluation of albedo enhancement to mitigate impacts of urban heat island in Rome (Italy) using WRF meteorological model. *Urban Clim.* **2018**, *24*, 551–566. [[CrossRef](#)]

**Disclaimer/Publisher’s Note:** The statements, opinions and data contained in all publications are solely those of the individual author(s) and contributor(s) and not of MDPI and/or the editor(s). MDPI and/or the editor(s) disclaim responsibility for any injury to people or property resulting from any ideas, methods, instructions or products referred to in the content.